J Mater Sci (2010) 45:5676–5684
DOI 10.1007/s10853-010-4633-y

Kinetics of isothermal reactive diffusion between solid Fe and liquid Al

Y. Tanaka · M. Kajihara

Received: 13 January 2010 / Accepted: 18 May 2010 / Published online: 4 June 2010

Abstract The kinetics of the reactive diffusion between solid Fe and liquid Al was experimentally observed using Fe/Al diffusion couples. The diffusion couples were prepared by an isothermal bonding technique and then immediately annealed in the temperature range of $T = 1053$–1093 K for various times up to $t = 600$ s. Owing to annealing, an intermetallic layer with a rather uniform thickness is produced at the Fe/Al interface in the diffusion couple and grows into the solid Fe specimen. The intermetallic layer consists of Fe_2Al_5 and $FeAl_3$, and the thickness is much smaller for $FeAl_3$ than for Fe_2Al_5. Hence, the growth of the intermetallic layer is predominantly governed by Fe_2Al_5. The total thickness, l, of the intermetallic layer increases with increasing annealing time, t, according to the parabolic relationship $l^2 = Kt$. This may mean that the growth of the intermetallic layer is controlled by volume diffusion. If the temperature dependence of the parabolic coefficient K is expressed by the equation $K = K_0\exp(-Q_K/RT)$, $K_0 = 126$ m^2/s and $Q_K = 248$ kJ/mol are obtained from the experimental values of K at $T = 1053$–1093 K by the least-squares method. A mathematical model was used to evaluate the interdiffusion coefficient, D, of Fe_2Al_5 from K. The evaluation provides $D_0 = 2.55 \times 10^3$ m^2/s and $Q = 259$ kJ/mol for the dependence of D on T described as $D = D_0\exp(-Q/RT)$. Thus, K is one fifth of D at $T = 1053$–1093 K, and Q_K does not necessarily coincide with Q. D is about two orders of magnitude greater for the values evaluated in the present study than for those extrapolated from the previously reported result at $T = 823$–913 K. The microstructure observation in a previous study suggests that such large values of D are attributed to the boundary diffusion in the intermetallic layer as well as the crystallographic anisotropy of Fe_2Al_5.

Y. Tanaka · M. Kajihara (✉)
Department of Materials Science and Engineering, Tokyo Institute of Technology, Yokohama 226-8502, Japan
e-mail: kajihara@materia.titech.ac.jp

Introduction

Aluminizing is one of the useful methods to improve the heat and corrosion resistance of steels. In this method, the steel is immersed in a molten Al bath for a certain period. During immersion, Fe–Al compounds with higher Al concentrations are formed at the interface between the steel and the molten Al due to the reactive diffusion. However, such Fe–Al compounds are brittle. Thus, the formation of the Fe–Al compounds deteriorates the mechanical properties on the surface of the steel. In order to control the formation of the compounds, the information on kinetics of the reactive diffusion is very important. Therefore, various efforts to obtain such information have been made by many investigators [1–11].

The reactive diffusion between liquid Al and solid Fe was experimentally studied by Bouché et al. [8]. In this experiment, Fe/Al diffusion couples were prepared by a melt bath technique and then isothermally annealed in the temperature range of $T = 973$–1173 K. A similar experiment was conducted by Bouayad et al. [10] In the binary Fe–Al system [12], $FeAl_3$, Fe_2Al_5, and $FeAl_2$ are the stable intermetallic compounds in this temperature range. According to their experimental results [8, 10], however, only Fe_2Al_5 and $FeAl_3$ are produced as visible layers at the Fe/Al interface in the diffusion couple during annealing. The thickness is much smaller for $FeAl_3$ than for Fe_2Al_5, and irregular tongue-like morphology is realized for Fe_2Al_5. Owing to the irregular morphology, the growth rate of Fe_2Al_5 could not be reliably determined in their experiments [8, 10].

Recently, the reactive diffusion between liquid Al and solid Fe was experimentally observed in a previous study [13]. In this experiment, Fe/Al diffusion couples were prepared by an isothermal bonding technique and then annealed at temperatures of $T = 973$–1073 K. After annealing, Fe_2Al_5 and $FeAl_3$ were observed, but $FeAl_2$ was not recognized clearly. Like the experiments by Bouché et al. [8] and Bouayad et al. [10], the Fe_2Al_5 layer shows the irregular tongue-like morphology at $T = 973$–1023 K. At $T = 1073$ K, however, Fe_2Al_5 is formed as a rather uniform layer. Thus, the morphology of Fe_2Al_5 varies depending on the annealing temperature. In the isothermal bonding technique [13], the Al melt and the solid Fe specimen are separately preheated at the same temperature as the annealing temperature in a vacuum. After sufficient preheating, the melt and the solid specimen are bonded with each other and then annealed immediately. Hence, in the isothermal bonding technique, the temperatures of the melt and the solid specimen are equivalent and remain constant during preheating, bonding, and annealing. As mentioned earlier, the observation in a previous study [13] indicates that the uniform Fe_2Al_5 layer is formed during isothermal annealing at $T = 1073$ K. At this temperature, however, the Fe_2Al_5 layer shows the irregular tongue-like morphology in the experiments with the melt bath technique [8, 10]. In the experiment by Bouché et al. [8], the solid Fe specimen was preheated above the Al melt in a vacuum chamber before immersion into the melt. Due to the temperature gradient in the chamber, however, the preheating temperature of the solid Fe specimen may be lower than the immersion temperature of the Al melt. In contrast, the preheating temperature of the solid Fe specimen was 473 K independent of the immersion temperature in the experiment by Bouayad et al. [10]. In both experiments [8, 10], the temperature of the solid Fe specimen continuously increases with increasing immersion time and then finally reaches to the immersion temperature. During continuous heating, Fe_2Al_5 is formed at the Fe/Al interface and grows into the solid Fe specimen. According to the observation in a previous study [13], however, the Fe_2Al_5 layer is uniform at $T = 1073$ K but irregular at $T < 1073$ K. Therefore, in the experiments with the melt bath technique [8, 10], the Fe_2Al_5 layer with the irregular tongue-like morphology is produced during continuous heating at $T < 1073$ K and then grows during isothermal annealing at $T = 1073$ K. Consequently, it is not so easy to obtain the uniform Fe_2Al_5 layer by the melt-bath technique. In order to examine the kinetics of the reactive diffusion between liquid Al and solid Fe, the isothermal bonding technique proposed in a previous study [14] was used to prepare diffusion couples consisting of liquid Al and solid Fe in the present study. The diffusion couple was isothermally annealed in the temperature range of $T = 1053$–1093 K, and then the growth behavior of Fe–Al compounds was observed in a metallographical manner. On the basis of the observation, the kinetics was quantitatively analyzed using the mathematical model reported in a previous study [15].

Experimental

Polycrystalline columnar specimens with a length of 5 mm were cut from a commercial rod of pure Fe with a diameter of 8 mm and purity of 99.7 % in a manner similar to a previous study [13]. The Fe rod contains a trace of C, 0.01 mass% of Si, 0.25 mass% of Mn, 0.004 mass% of P, 0.004 mass% of S, 0.01 mass% of Cu, 0.01 mass% of Ni, and 0.01 mass% of Cr as impurities. The columnar specimens were separately annealed in evacuated silica capsules at a temperature of 1173 K for a time of 2 h, followed by air cooling without breaking the capsules. The top and bottom flat-surfaces of each annealed columnar specimen were mechanically polished on 800-4000 emery papers.

A commercial rod of pure Al with a diameter of 6 mm and purity of 99.99 % was cut into columnar specimens with a length of 9.6 mm. Each polished Fe specimen was encapsulated together with a columnar Al specimen in an evacuated silica capsule with an inner diameter of 8.5 mm. The silica capsule was isothermally preheated for a time of 1.8 ks (30 min) in the temperature range between 1053 K and 1093 K. During preheating, the solid Fe specimen was separated from the Al melt in the silica capsule. After preheating, a flat surface of the solid Fe specimen was immediately contacted with that of the Al melt with a diameter of 8.5 mm and a length of 4.8 mm to prepare a columnar Fe/Al diffusion couple. The diffusion couple was isothermally annealed for various times up to 600 s (10 min) at the same temperature as preheating, followed by water quenching with breaking the capsule. The annealing temperature and time are denoted by T and t, respectively.

Cross-sections of the annealed diffusion couple were mechanically polished on 800-4000 emery papers and then finished using diamond with a diameter of 1 μm. The microstructure of the cross-section was observed with a back-scattered electron image (BEI) by scanning electron microscopy (SEM). Concentrations of Fe and Al in each phase on the cross-section were measured by electron probe microanalysis (EPMA) using pure Fe and Al with purity of 99.99 % as standard specimens under the following conditions: the accelerating voltage was 20 kV; the probe current was 5 nA; the analyzing crystals for Fe-K_α and Al-K_α were lithium fluoride (LiF) and thallium acid phthalate (TAP), respectively; and the chemical composition was evaluated by a standard ZAF correction technique.

Model

In order to analyze quantitatively the kinetics of the reactive diffusion controlled by volume diffusion, a hypothetical binary A–B system consisting of one intermetallic compound and two primary solid solution phases was adopted in previous studies [15–22]. The α and γ phases are the primary solid solution phases of components A and B, respectively, and the β phase is the intermetallic compound. Now, we consider a semi-infinite diffusion couple composed of the α and γ phases with initial compositions of $y^{\alpha 0}$ and $y^{\gamma 0}$, respectively. Here, y is the mol fraction of component B. In the semi-infinite diffusion couple, the thickness is semi-infinite for the α and γ phases, and the α/γ interface is flat. Therefore, the interdiffusion of components A and B occurs unidirectionally along the direction perpendicular to the flat interface. This direction is called the diffusional direction. If the diffusion couple is annealed at temperature T for an appropriate time, the β phase will be formed as a layer with a uniform thickness along the interface owing to the reactive diffusion between the α and γ phases. The concentration profile of component B across the β phase layer along the diffusional direction is schematically drawn in Fig. 1 [15]. In this figure, the ordinate shows the mol fraction y, and the abscissa indicates the distance x measured from the initial position of the α/γ interface. Dashed lines and solid curves show the concentration profiles before and after annealing, respectively, and $z^{\alpha\beta}$ and $z^{\beta\gamma}$ indicate the positions of the α/β and β/γ interfaces, respectively, after annealing. When the local equilibrium is realized at each migrating interface during annealing, the compositions of the neighboring phases at the interface coincide with those of the corresponding phase boundaries at temperature T in the phase diagram of the binary A–B system. Consequently, the migration of the interface is controlled by the volume diffusion in the neighboring phases. In Fig. 1, $y^{\alpha\beta}$ and $y^{\beta\alpha}$ are the compositions of the α and β phases, respectively, at the α/β interface, and $y^{\beta\gamma}$ and $y^{\gamma\beta}$ are those of the β and γ phases, respectively, at the β/γ interface. The compositions $y^{\alpha\beta}$, $y^{\beta\alpha}$, $y^{\beta\gamma}$, and $y^{\gamma\beta}$ give the boundary conditions, and those $y^{\alpha 0}$ and $y^{\gamma 0}$ provide the initial conditions.

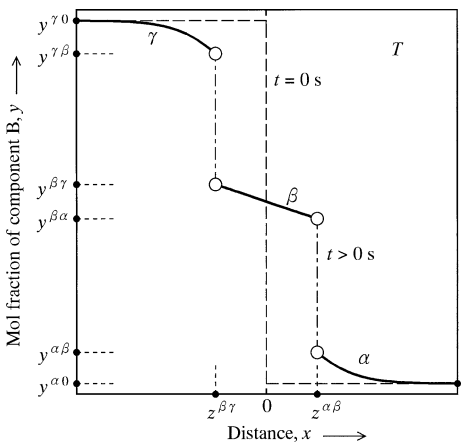

Fig. 1 Concentration profile of component B across the β phase along the diffusional direction in the semi-infinite diffusion couple [15]

For the reactive diffusion controlled by volume diffusion, the positions $z^{\alpha\beta}$ and $z^{\beta\gamma}$ of the α/β and β/γ interfaces are described as functions of the annealing time, t, by the equations

$$z^{\alpha\beta} = K^{\alpha\beta}\sqrt{4D^{\alpha}t} = K^{\beta\alpha}\sqrt{4D^{\beta}t} \tag{1a}$$

and

$$z^{\beta\gamma} = K^{\beta\gamma}\sqrt{4D^{\beta}t} = K^{\gamma\beta}\sqrt{4D^{\gamma}t}, \tag{1b}$$

respectively [23]. Here, D^{α}, D^{β}, and D^{γ} are the interdiffusion coefficients for volume diffusion in the α, β, and γ phases, respectively, and $K^{\alpha\beta}$, $K^{\beta\alpha}$, $K^{\beta\gamma}$, and $K^{\gamma\beta}$ are dimensionless coefficients. The thickness, l, of the β phase layer is determined as the difference between $z^{\alpha\beta}$ and $z^{\beta\gamma}$, and thus the following equation is obtained from Eq. 1a, 1b to express l as a function of t.

$$l^2 = \left(z^{\alpha\beta} - z^{\beta\gamma}\right)^2 = 4D^{\beta}\left(K^{\beta\alpha} - K^{\beta\gamma}\right)^2 t = Kt \tag{2}$$

Equation 2 indicates the parabolic relationship, where K is the parabolic coefficient with a dimension of m^2/s. According to Eq. 2, K is described as a function of D^{β}, $K^{\beta\alpha}$, and $K^{\beta\gamma}$ by the following equation:

$$K \equiv 4D^{\beta}\left(K^{\beta\alpha} - K^{\beta\gamma}\right)^2. \tag{3}$$

The dimensionless coefficients are related to the initial and boundary conditions as follows [15]:

$$c^{\beta\alpha} - c^{\alpha\beta} = \frac{c^{\alpha 0} - c^{\alpha\beta}}{K^{\alpha\beta}\sqrt{\pi}\{1 - \mathrm{erf}(K^{\alpha\beta})\}}\exp\left\{-\left(K^{\alpha\beta}\right)^2\right\} + \frac{c^{\beta\gamma} - c^{\beta\alpha}}{K^{\beta\alpha}\sqrt{\pi}\{\mathrm{erf}(K^{\beta\alpha}) - \mathrm{erf}(K^{\beta\gamma})\}}\exp\left\{-\left(K^{\beta\alpha}\right)^2\right\} \tag{4a}$$

and

$$c^{\gamma\beta} - c^{\beta\gamma} = \frac{c^{\beta\alpha} - c^{\beta\gamma}}{K^{\beta\gamma}\sqrt{\pi}\{\mathrm{erf}(K^{\beta\alpha}) - \mathrm{erf}(K^{\beta\gamma})\}}\exp\left\{-\left(K^{\beta\gamma}\right)^2\right\} + \frac{c^{\gamma 0} - c^{\gamma\beta}}{K^{\gamma\beta}\sqrt{\pi}\{1 + \mathrm{erf}(K^{\gamma\beta})\}}\exp\left\{-\left(K^{\gamma\beta}\right)^2\right\}. \tag{4b}$$

Here, c is the concentration of component B measured in mol per unit volume. The initial and boundary conditions are indicated with the concentration c in Eq. 4a, 4b but shown with the mol fraction y in Fig. 1. However, y is

readily converted into c by the equation $c = y/V_m$, where V_m is the molar volume of the relevant phase. The following relationships are deduced from Eq. 1a, 1b:

$$K^{\alpha\beta} = K^{\beta\alpha}\sqrt{\frac{D^{\beta}}{D^{\alpha}}} \tag{5a}$$

and

$$K^{\gamma\beta} = K^{\beta\gamma}\sqrt{\frac{D^{\beta}}{D^{\gamma}}}. \tag{5b}$$

Equation 5a, 5b indicates that only two of the four dimensionless coefficients are independent. In the present study, $K^{\beta\alpha}$ and $K^{\beta\gamma}$ are chosen as the independent variables. Insertion of Eq. 5a, 5b into Eq. 4a, 4b yields two independent equations. As a result, the two independent variables are determined from the two independent equations, and then K is finally calculated from Eq. 3.

Results and discussion

Microstructure

Typical BEI micrographs of the cross-section for various diffusion couples are shown in Fig. 2. Figure 2a, b indicates the micrographs of the diffusion couples annealed at $T = 1053$ K and 1093 K, respectively, for $t = 600$ s (10 min). In this figure, the brightest region on the lower side is the Fe specimen, and the darkest region on the upper side is the Al specimen. As can be seen, a compound layer with an intermediate contrast is observed between the Fe and Al specimens. Concentration profiles of Fe and Al across the compound layer were measured by EPMA. A result for the diffusion couple with $T = 1083$ K and $t = 300$ s (5 min) is shown in Fig. 3. In this figure, the ordinate and the abscissa indicate the mol fraction y_i of component i and the distance x, respectively, and open circles and squares show the mol fractions y_{Al} and y_{Fe}, respectively. According to the result in Fig. 3, the compound layer consists of Fe_2Al_5 and $FeAl_3$. However, the thickness is much smaller for $FeAl_3$ than for Fe_2Al_5. Since Fe_2Al_5 and $FeAl_3$ are brittle, cracks are formed in the compound layer on the cross-section during mechanical polishing as shown in Fig. 2. In optical micrographs, $FeAl_3$ is distinguished from Fe_2Al_5 [13]. As indicated in Fig. 3, however, the thickness is much smaller for $FeAl_3$ than for Fe_2Al_5. Hence, the thickness of $FeAl_3$ was not necessarily reliably determined from the optical micrograph. In contrast, the mean atomic number is close to each other between Fe_2Al_5 and $FeAl_3$. Thus, Fe_2Al_5 and $FeAl_3$ are not clearly distinguishable in the BEI micrographs like Fig. 2. In Fig. 2, the black and gray areas in the Al specimen are the Al-rich solid-solution (Al) phase and $FeAl_3$,

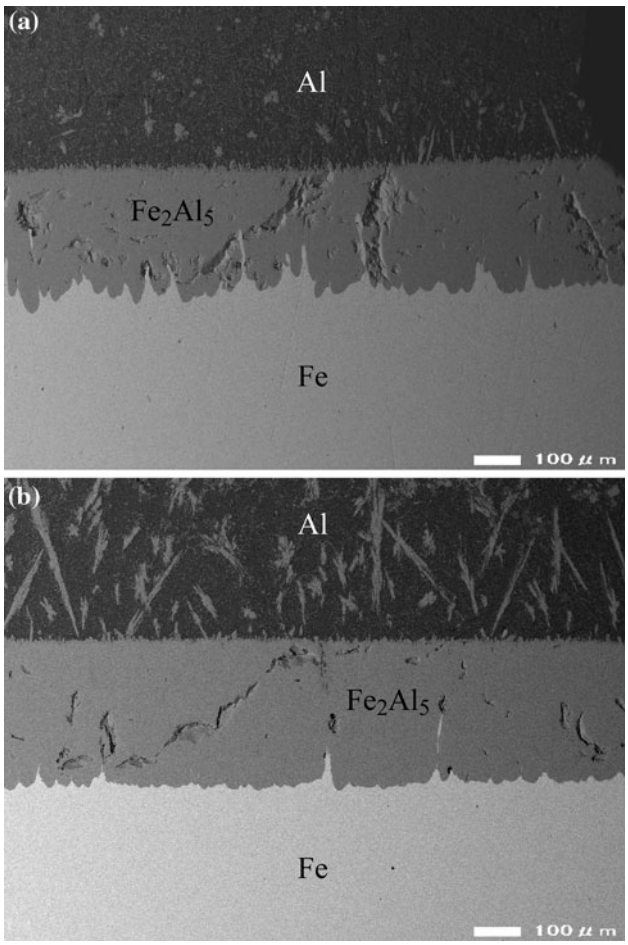

Fig. 2 Back-scattered electron images of cross-section for the Fe/Al diffusion couples annealed for $t = 600$ s (10 min) at **a** $T = 1053$ K and **b** $T = 1093$ K

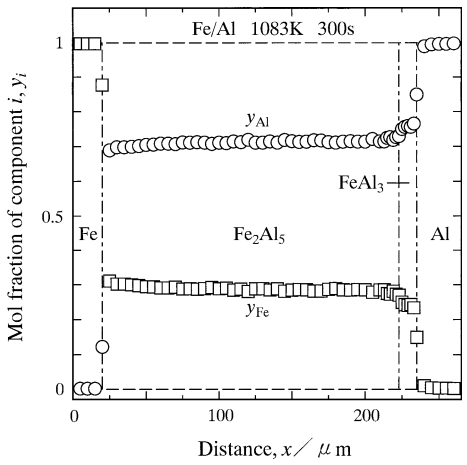

Fig. 3 Concentration profiles of Fe and Al across the intermetallic layer in the Fe/Al diffusion couple annealed at $T = 1083$ K for $t = 300$ s (5 min)

respectively. During cooling after isothermal annealing in the liquid single-phase region, the Al-rich liquid-solution (L) phase containing a certain amount of Fe is decomposed into the Al phase and $FeAl_3$ by the eutectic reaction $L \rightarrow Al + FeAl_3$, where the eutectic temperature is 928 K [12]. The BEI micrographs in Fig. 2 suggest that the eutectic reaction occurs very fast even during water quenching. The volume fraction of $FeAl_3$ in the Al specimen increases with increasing annealing temperature and time. According to a recent phase diagram in the binary Fe–Al system [12], $FeAl_2$ as well as Fe_2Al_5 and $FeAl_3$ should appear as a stable intermetallic compound at $T = 1053$–1093 K. However, $FeAl_2$ was not observed in any diffusion couples in the present study. Hence, nucleation and/or growth may be much slower for $FeAl_2$ than for Fe_2Al_5 and $FeAl_3$. As a consequence, $FeAl_2$ cannot grow to visible thicknesses within the experimental annealing times. Microstructures similar to Fig. 2 were observed for all the diffusion couples.

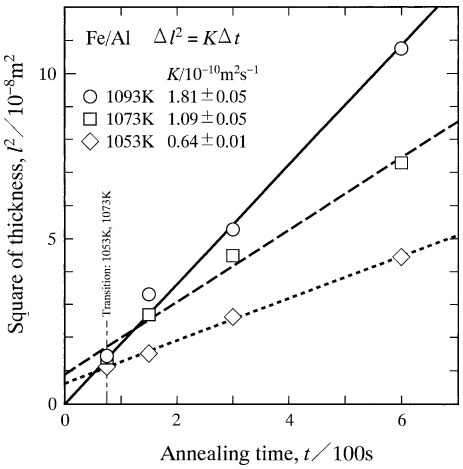

Fig. 4 The square of the thickness l of the intermetallic layer versus the annealing time t for the Fe/Al diffusion couple at $T = 1053$ K, 1073 K, and 1093 K shown as *open rhombuses*, *squares*, and *circles*, respectively. A *solid line* indicates the calculation from Eq. 7 and *dotted* and *dashed lines* show those from Eq. 8

Growth behavior of intermetallic layer

In the BEI micrographs of the cross-section like Fig. 2, the compound layer is clearly distinguishable from the Fe and Al specimens. Furthermore, the compound layer possesses the morphology of a rather uniform thickness. Hereafter, the compound layer with the uniform morphology is called the intermetallic layer. From the BEI micrograph, the mean thickness, l, of the intermetallic layer was evaluated by the following equation [13]:

$$l = \frac{A}{w}. \tag{6}$$

Here, A and w are the total area and the total length of the intermetallic layer, respectively, on the cross-section. At each annealing time, l was calculated from Eq. 6 using the total values of A and w for various cross-sections. The results of $T = 1053$ K, 1073 K, and 1093 K are plotted as open rhombuses, squares, and circles, respectively, in Fig. 4. In this figure, the ordinate shows the square of the thickness l, and the abscissa indicates the annealing time t. As to the result of $T = 1093$ K, the open circles lie well on a solid line. This means that the parabolic relationship holds between the thickness, l, and the annealing time, t, as follows:

$$l^2 = Kt. \tag{7}$$

From the open circles in Fig. 4, the parabolic coefficient K was estimated for $T = 1093$ K by the least-squares method. The solid line shows the calculation from Eq. 7 with the estimated value of K. Also for the results of $T = 1053$ K and 1073 K, the open rhombuses and squares are located well on dotted and dashed fitting-lines, respectively. However, the dotted and dashed lines intersect the ordinate with $l > 0$ at $t = 0$. This implies that the transition of the rate-controlling process from boundary diffusion to volume diffusion occurs at the critical annealing time t_c [24]. It is recommended by van Loo [24] that the parabolic relationship at $t > t_c$ should be described by the following equation instead of Eq. 7.

$$l^2 - l_c^2 = K(t - t_c) \tag{8}$$

Here, l_c is the value of l at $t = t_c$. According to the recommendation, K is evaluated from Eq. 8 even at $T = 1053$ K and 1073 K. Unfortunately, however, t_c cannot be reliably determined from the open rhombuses and squares in Fig. 4. Hence, for convenience' sake, it is assumed that t_c is equal to the shortest annealing time of $t_s = 75$ s. The values of l_c^2 for $t_c = t_s$ were obtained from the fitting-lines in Fig. 4 and listed at the seventh column in Table 1. With these values of l_c^2 and t_c, K was evaluated from Eq. 8 at $T = 1053$ K and 1073 K using the open rhombuses and squares, respectively, by the least-squares method. The evaluated values of K are shown in Fig. 4. When the growth of the intermetallic layer is controlled by

Table 1 The interface compositions $y^{\alpha\beta}$, $y^{\beta\alpha}$, $y^{\beta\gamma}$, and $y^{\gamma\beta}$ [12] and the parameters t_c and l_c^2 at each annealing temperature

T/K	$y^{\alpha\beta}$	$y^{\beta\alpha}$	$y^{\beta\gamma}$	$y^{\gamma\beta}$	t_c/s	$l_c^2/10^{-8}m^2$
1053	0.499	0.700	0.730	0.971	75	1.10
1073	0.500	0.700	0.730	0.967	75	1.71
1093	0.502	0.700	0.730	0.962	0	0

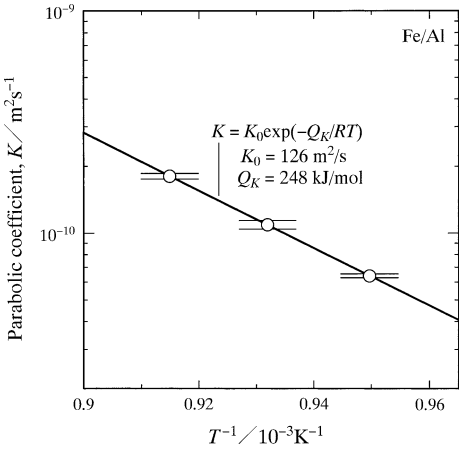

Fig. 5 The parabolic coefficient K versus the reciprocal of the temperature T. A *straight line* indicates the calculation from Eq. 9

volume diffusion, the parabolic relationship holds between l and t as mentioned above. However, the parabolic relationship is realized also for the growth controlled by boundary diffusion unless grain growth occurs in any phases of the diffusion couple [25]. Therefore, the parabolic relationship provides two possibilities of the rate-controlling process for the growth of the intermetallic layer. As reported in a previous study [13], the intermetallic layer consists of columnar blocks and each columnar block is composed of equiaxed grains. Since the columnar block coarsens during annealing, the parabolic relationship may indicate the volume diffusion rate-controlling process.

The values of K are plotted against the annealing temperature T as open circles with error bars in Fig. 5. In this figure, the ordinate shows the logarithm of K, and the abscissa indicates the reciprocal of T. The temperature dependence of K is expressed by the following equation with certain accuracy [16–18]:

$$K = K_0 \exp\left(-\frac{Q_K}{RT}\right). \tag{9}$$

Here, K_0 is the pre-exponential factor, and Q_K is the activation enthalpy. From the open circles in Fig. 5, K_0 and Q_K were estimated by the least-squares method as shown with a solid line. As can be seen, the open circles are located well on the solid line. As a consequence, Eq. 9 satisfactorily describes the dependence of K on T within the experimental uncertainty.

Analysis of kinetics

As previously mentioned, the intermetallic layer is composed of Fe_2Al_5 and $FeAl_3$. According to the result in Fig. 3, however, the thickness is much smaller for $FeAl_3$ than for Fe_2Al_5. This means that the growth of the intermetallic layer is predominantly governed by Fe_2Al_5. Hence, in order to simplify the analysis, it is assumed that the intermetallic layer consists of only Fe_2Al_5. The interdiffusion coefficient D^θ of the θ phase is expressed as a function of the temperature T by the following equation of the same formula as Eq. 9.

$$D^\theta = D_0^\theta \exp\left(-\frac{Q^\theta}{RT}\right) \tag{10}$$

Like K_0 and Q_K in Eq. 9, D_0^θ and Q^θ are the pre-exponential factor and the activation enthalpy, respectively. Hereafter, the Fe-rich solid-solution phase with the body-centered cubic (bcc, $A2$) or $B2$ structure and the Al-rich liquid-solution phase are denoted by $\theta = \alpha$ and L, respectively. For simplicity, however, the superscript is omitted for Fe_2Al_5. Since the solubility y_{Fe}^L of Fe in the L phase is 0.029–0.038 at T = 1053–1093 K [12], respectively, D^L is almost equal to the self diffusion coefficient D_{Fe}^L of Fe in the L phase. Various values of D_{Fe}^L were reported by many investigators [26–29]. Their values are shown as different open symbols with solid lines in Fig. 6. In this figure, D_{Fe}^L is simply denoted by D^L, and the ordinate and the abscissa indicate the logarithm of D^L and the reciprocal of T, respectively. As can be seen, there are large discrepancies among the values of D^L reported by the different investigators. In the temperature range of T = 1053–1093 K, D^L is more than one order of magnitude greater for the largest value than for the smallest value. Du et al. [30] critically reviewed such discrepancies of D^L and then concluded that the values reported by Eremenko et al. [27] and Ejima et al. [28] were reliable. Using the selected values [27, 28], Du et al. [30] revaluated $D_0^L = 2.34 \times 10^{-7}$ m²/s and $Q^L = 35.0$ kJ/mol for D^L. The revaluated result is shown as open inverse-triangles with a dashed line in Fig. 6. On the other hand, the solubility y_{Al}^α of Al in the α phase is 0.499–0.502 at T = 1053–1093 K, respectively. Thus,

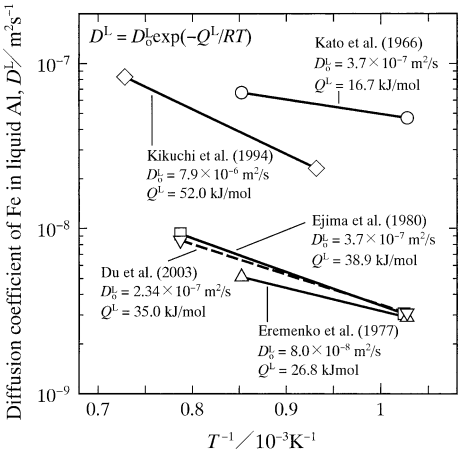

Fig. 6 The diffusion coefficient D^L versus the reciprocal of the temperature T reported by various researchers [26–30]

unlike y^{L}_{Fe}, y^{α}_{Al} is not sufficiently small. Furthermore, the crystal structure of the α phase is bcc (*A2*) at lower Al concentrations but *B2* at higher Al concentrations [12]. Hence, D^{α} may not be necessarily close to the self diffusion coefficient D^{α}_{Al} of Al in the α phase in the full composition range of the α single-phase region. Nevertheless, D^{α} is much smaller than D^{L} and D. In such a case, the growth rate of Fe_2Al_5 is insensitive to D^{α} [15]. Therefore, in the present analysis, it is assumed that D^{α} is equal to D^{α}_{Al}. According to this assumption, the following values were adopted for D^{α}: $D^{\alpha}_0 = 5.2 \times 10^{-4}$ m^2/s and $Q^{\alpha} =$ 246 kJ/mol [31].

As mentioned earlier, the mol fraction y is readily converted into the concentration c by the equation $c = y/V_m$. Here, V_m is the molar volume of the relevant phase. The molar volumes V^{L}_m and V^{α}_m of the pure L and α phases are 11.17×10^{-6} m^3/mol and 7.29×10^{-6} m^3/mol, respectively, at $T = 933$ K [31]. Thus, V^{L}_m is 53% greater than V^{α}_m. On the other hand, at $T = 1053$–1093 K, D^{L} is more than three orders of magnitude greater than D^{α}. Although K is a function of the diffusion coefficients and the molar volumes of the constituent phases through the equation $c = y/V_m$ and Eqs. 3–5a, 5b under the initial and boundary conditions described with y, the difference between V^{L}_m and V^{α}_m is negligible compared with that between D^{L} and D^{α}. Thus, with sufficient accuracy, we may assume that the molar volumes of all the constituent phases are equivalent. On the basis of this assumption, the concentration c in Eq. 4a, 4b is automatically replaced with the mol fraction y. In the Fe/Al diffusion couple, the components A and B are Fe and Al, respectively, and the superscripts α, β, and γ in Eqs. 1a, 1b–5a, 5b correspond to the α phase, Fe_2Al_5, and the L phase, respectively. The initial compositions of the Fe and Al specimens in the diffusion couple are given as $y^{\alpha 0} = 0$ and $y^{\gamma 0} = 1$, respectively. The composition $y^{\alpha\beta}$ represents the solubility of Al in the α phase, and hence $y^{\alpha\beta} = y^{\alpha}_{Al}$. On the other hand, $y^{\beta\alpha}$ and $y^{\beta\gamma}$ show the lowest and highest concentrations of Al in the solubility range of Fe_2Al_5, and $y^{\gamma\beta}$ indicates the concentration of Al on the liquidus curve of the L phase. Thus, $y^{\gamma\beta} = 1 - y^{L}_{Fe}$. The interface compositions $y^{\alpha\beta}$, $y^{\beta\alpha}$, $y^{\beta\gamma}$ and $y^{\gamma\beta}$ at $T = 1053$–1093 K [12] are listed in Table 1.

Using the parameters mentioned above, D was evaluated from Eqs. 3–5a, 5b for the values of D^{L} indicated with the different open symbols in Fig. 6 to reproduce the experimental values of K at $T = 1053$–1093 K in Figs. 4 and 5. The results are shown in Fig. 7 with the same open symbols as Fig. 6. As can be seen, D is smaller than D^{L} but much greater than D^{α}. Furthermore, like Fig. 6, there are discrepancies of D among the different open symbols. Nevertheless, in Fig. 7, D is merely about twice greater for the largest value than for the smallest value. Since D^{L} is greater than D as mentioned above, K varies depending on

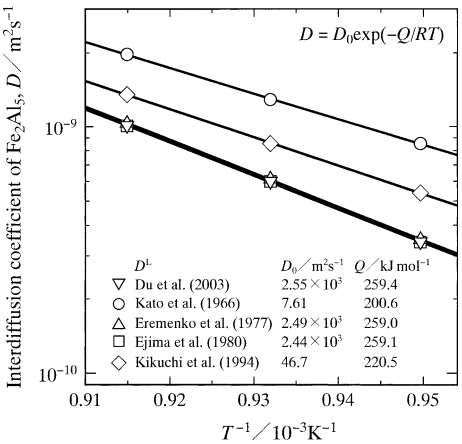

Fig. 7 The diffusion coefficient D versus the reciprocal of the temperature T evaluated from Eqs. 3–5a, 5b using D^{L} shown in Fig. 6

D^{L} and D [15]. Even in such a case, however, K is not so sensitive to D^{L} [15]. As a result, the evaluation of D is not strongly affected by the discrepancy of D^{L}.

The reactive diffusion between solid Fe and solid Al was experimentally observed in a previous study [32]. In this experiment, Al/Fe/Al diffusion couples were prepared by a diffusion bonding technique and then isothermally annealed at $T = 823$–913 K for various periods up to $t = 4.32$ ks (120 h). During annealing, a Fe_2Al_5 layer is formed at the Fe/Al interface in the diffusion couple and grows according to the parabolic relationship. However, $FeAl_3$ and $FeAl_2$ were not clearly observed even after the longest annealing at each temperature. In the solid-Fe/solid-Al reactive diffusion, coarse equiaxed grains of Fe_2Al_5 are formed by isothermal annealing at $T = 823$–913 K [32]. Hence, the growth of the intermetallic layer is governed by volume diffusion. On the other hand, in the solid-Fe/liquid-Al reactive diffusion, columnar blocks of Fe_2Al_5 are produced in the early stages and then coarsen during isothermal annealing at $T = 973$–1073 K [13]. Here, the columnar block is composed of equiaxed grains. As a result, at $T = 1053$–1073 K, the growth of the intermetallic layer may be controlled by boundary diffusion in the early stages but by volume diffusion in the late stages. In a previous study [19], D was evaluated from the experimental values of K at $T = 823$–913 K in a manner similar to the present study. The evaluation is shown as open squares with a dashed line in Fig. 8. In this figure, the open inverse-triangles with a solid line in Fig. 7 are represented as open circles with a solid line. The penetration distance, p, of Fe into the L phase from the α phase in the Fe/Al diffusion couple during isothermal annealing is roughly estimated by the following equation [15]:

$$p = 2\sqrt{D^{L}t}. \tag{11}$$

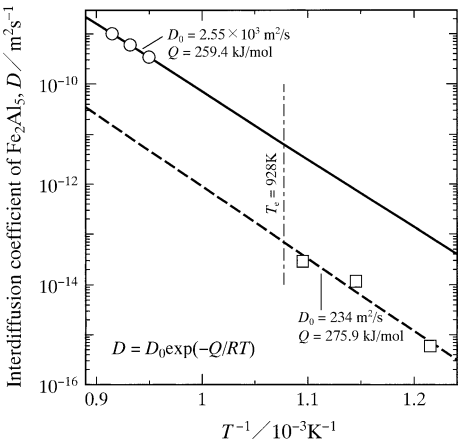

Fig. 8 The *open inverse-triangles* with a solid line in Fig. 7 are represented as *open circles* with a *solid line*. The corresponding result in a previous study [19] is shown as *open squares* with a *dashed line*

Using the parameters $D_0^{\mathrm{L}} = 2.34 \times 10^{-7}$ m²/s and $Q^{\mathrm{L}} = 35.0$ kJ/mol, reported by Du et al. [30], we obtain $D^{\mathrm{L}} = 4.30 \times 10^{-9}$ m²/s, 4.63×10^{-9} m²/s, and 4.97×10^{-9} m²/s at $T = 1053$ K, 1073 K, and 1093 K, respectively, from Eq. 10. On the other hand, the longest annealing time, t_{m}, is 600 s at $T = 1053$–1093 K. Thus, $p = 3.2$ mm, 3.3 mm, and 3.5 mm are estimated for $T = 1053$ K, 1073 K, and 1093 K, respectively, at $t = t_{\mathrm{m}}$ from Eq. 11. As mentioned in the "Experimental" section, the length s_{Al} of the L phase and that s_{Fe} of the α phase are 4.8 and 5 mm, respectively, for the Fe/Al diffusion couple. Since p is smaller than s_{Al} at $t = t_{\mathrm{m}}$, the Fe/Al diffusion couple is considered semi-infinite within the experimental annealing times. Owing to preheating before annealing, the temperature becomes uniform in both the L and α phases. Thus, thermal convection is minimized in the L phase during annealing. On the other hand, the circular side of the L phase is directly contacted with the inner side of the silica capsule. Hence, the flat surface is the only free surface of the L phase. Since the flat free-surface of the L phase is parallel to the Fe/Al interface in the diffusion couple and the thermal convection is negligible, the chemical composition as well as the temperature should be uniform along the flat free-surface during annealing. Therefore, Marangoni convection is minimized for the flat free-surface. In contrast, the L-phase/silica interface is not microscopically smooth. It may be difficult for Marangoni convection to occur readily along such a microscopically uneven interface. Consequently, we may expect that Marangoni convection is also negligible in the L phase. In previous studies [14, 33], it was confirmed that the penetration of Cu into the L phase in the solid-Cu/liquid-Al reactive diffusion was actually controlled by volume diffusion. In the solid-Fe/liquid-Al reactive diffusion, however, the L phase is quickly decomposed into the Al-rich solid-solution (Al) phase and $FeAl_3$ by the eutectic reaction $L \rightarrow Al + FeAl_3$ during water quenching as mentioned earlier. Furthermore, the solubility of Fe in the Al phase is negligible [12]. As a consequence, the penetration of Fe into the L phase during isothermal annealing could not be experimentally ascertained from the concentration profiles like Fig. 3. Nevertheless, the result of the solid-Cu/liquid-Al reactive diffusion [14, 33] guarantees that volume diffusion is the rate-controlling process also for the penetration of Fe into the L phase in the solid-Fe/liquid-Al reactive diffusion. Thus, like the analysis in a previous study [19], the mathematical model [15] used in the present study is valid for the evaluation of D. In the temperature range of $T = 1053$–1093 K, D is about two orders of magnitude greater for the solid line than for the dashed line in Fig. 8. Recently, Nishimoto et al. [11] experimentally observed the solid-Fe/liquid-Al reactive diffusion. In their experiment, Fe/Al diffusion couples were prepared by the melt bath technique and then annealed at $T = 1023$ K for various times up to $t = 600$ s. Like other experiments [8, 10, 13], the irregular tongue-like Fe_2Al_5 layer was observed in the annealed diffusion couples. Using such diffusion couples, the crystallographic orientation relationship of the polycrystalline grain in the Fe_2Al_5 layer was measured by an electron back-scattered diffraction (EBSD) technique. Here, Fe_2Al_5 possesses the orthorhombic crystal structure with lattice parameters of $a = 0.76573$ nm, $b = 0.64087$ nm, and $c = 0.42265$ nm [34]. The EBSD measurement indicates that each tongue is a columnar block consisting of fine equiaxed grains. The c-axis of the fine equiaxed grain is almost perpendicular to the initial Fe/Al interface but the a- and b-axes are randomly distributed on a plane mostly parallel to the Fe/Al interface. Although Fe_2Al_5 is formed as a rather uniform layer at $T = 1053$–1093 K in the present study, the observation in a previous study [13] indicates that the uniform layer consists of columnar blocks and each columnar block is composed of fine equiaxed grains. Thus, according to the EBSD measurement by Nishimoto et al. [11], we can expect that the c-axis of each fine equiaxed grain is almost perpendicular to the initial Fe/Al interface. As a consequence, the solid line in Fig. 8 may show the value of D along the c-axis. On the other hand, the observation at $T = 823$–913 K in a previous study [32] indicates that the Fe_2Al_5 layer consists of coarse equiaxed grains. Unlike the fine equiaxed grains in the columnar block, any preferential growth directions are not recognized for the coarse equiaxed grains. Therefore, the dashed line in Fig. 8 may correspond to a mean of D among the a-, b-, and c-axes. Due to the orthorhombic crystal structure of Fe_2Al_5, there exists anisotropy for D [3]. The comparison between the solid and dashed lines in Fig. 8 implies that D is more than two orders of magnitude greater along the c-axis than along the a- and b-axes.

As mentioned earlier, however, the columnar block of the Fe_2Al_5 layer is composed of fine equiaxed grains. In a previous study [13], coarsening was experimentally examined for the columnar block but not for the fine equiaxed grain. If the coarsening of the fine equiaxed grain is sluggish in the late stages, the parabolic relationship holds between l and t even for the growth of the Fe_2Al_5 layer controlled by boundary diffusion [25]. In such a case, the boundary diffusion as well as the crystallographic anisotropy contributes to the values of D shown as the open circles in Fig. 8. This may be the reason why D is about two orders of magnitude greater for the solid line than for the dashed line in Fig. 8.

Conclusions

In order to examine the kinetics of the reactive diffusion in the liquid-Al/solid-Fe system, Fe/Al diffusion couples were prepared by the isothermal bonding technique and then immediately annealed at temperatures of $T = 1053$–1093 K. At these temperatures, $FeAl_3$, Fe_2Al_5, and $FeAl_2$ are the stable intermetallic compounds in the binary Fe–Al system [12]. During annealing, however, only Fe_2Al_5 and $FeAl_3$ are formed as visible layers at the Fe/Al interface in the diffusion couple. The intermetallic layer consisting of Fe_2Al_5 and $FeAl_3$ indicates the morphology with a rather uniform thickness and grows into the solid Fe specimen. Since the thickness is much smaller for $FeAl_3$ than for Fe_2Al_5, the growth of the intermetallic layer is dominated by Fe_2Al_5. The square of the total thickness of the intermetallic layer is proportional to the annealing time. Such annealing time dependence of the thickness is called the parabolic relationship. The parabolic relationship may usually indicate that the growth is controlled by volume diffusion. The mathematical model reported in a previous study [15] was used to evaluate the interdiffusion coefficient D of Fe_2Al_5 from the experimental values of the parabolic coefficient. The values of D evaluated at $T = 1053$–1093 K are about two orders of magnitude greater than those extrapolated from the result at $T = 823$–913 K reported in a previous study [32]. The microstructure observation in a previous study [13] implies that the boundary diffusion across the intermetallic layer as well as the crystallographic anisotropy of orthorhombic Fe_2Al_5 contributes to the evaluation of D.

Acknowledgements The authors are grateful to Professor M. Takeyama at Tokyo Institute of Technology, Japan for stimulating discussions. The present study was supported by a Grant-in-Aid for Scientific Research from the Ministry of Education, Culture, Sports, Science and Technology of Japan.

References

1. Gebhardt E, Obrowski W (1953) Z Metallkde 44:154
2. Gürtler G, Sagel K (1955) Z Metallkde 46:738
3. Heumann T, Dittrich S (1959) Z Metallkde 50:617
4. Denner SG, Jones RD (1977) Met Technol 4:167
5. Yeremenko VN, Natanzon YV, Dybkov VI (1981) J Mater Sci 16:1748. doi:10.1007/BF00540620
6. Eggeler G, Auer W, Kaesche H (1986) Z Metallkde 77:239
7. Dybkov VI (1990) J Mater Sci 25:3615. doi:10.1007/BF00575397
8. Bouché K, Barbier F, Coulet A (1998) Mater Sci Eng A 249:167
9. Kobayashi S, Yakou T (2002) Mater Sci Eng A 338:44
10. Bouayad A, Gerometta Ch, Belkebir A, Ambari A (2003) Mater Sci Eng A 363:53
11. Nishimoto S, Kobayashi S, Takada N, Matsuo T, Takeyama M (2008) Abst Annual Meeting JIM, Kumamoto, Japan, Sep. 23–25, p 82
12. Massalski TB, Okamoto H, Subramanian PR, Kacprzak L (1990) Binary alloy phase diagrams, vol 1. ASM International, Materials Park, Ohio, p 148
13. Tanaka Y, Kajihara M (2009) Mater Trans 50:2212
14. Tanaka Y, Kajihara M, Watanabe Y (2006) Mater Sci Eng A 445–446:355
15. Kajihara M (2004) Acta Mater 52:1193
16. Kajihara M (2005) Mater Sci Eng A 403:234
17. Kajihara M (2005) Mater Trans 46:2142
18. Kajihara M (2006) Defect Diffus Forum 249:91
19. Kajihara M (2006) Mater Trans 47:1480
20. Tanaka Y, Kajihara M (2006) Mater Trans 47:2480
21. Kajihara M, Yamashina T (2007) J Mater Sci 42:2432. doi:10.1007/s10853-006-1212-3
22. Kajihara M (2008) Mater Trans 49:715
23. Jost W (1960) Diffusion of solids, liquids, gases. Academic Press, New York, p 68
24. van Loo FJJ (1990) Prog Solid State Chem 20:47
25. Furuto A, Kajihara M (2008) Mater Trans 49:294
26. Kato M, Kosaka M, Yamada M, Takayanagi T, Minowa S (1966) Report of Nagoya Municipal Industrial Research Institute 15:301
27. Eremenko VN, Natanzon YV, Tivov VP (1977) Russ Metall 2:77
28. Ejima T, Yamamura T, Uchida N, Matsuzaki Y, Nikaido M (1980) J Jpn Inst Met 44:316
29. Kikuchi T, Tani K (1994) Trans Niihama Coll Technol 30:65
30. Du Y, Chang YA, Huang B, Gong W, Jin Z, Xu H, Yuan Z, Liu Y, He Y, Xie FY (2003) Mater Sci Eng A 363:140
31. Japan Institute of Metals (1993) (ed) Metals data book. Maruzen, Tokyo, p 21
32. Naoi D, Kajihara M (2007) Mater Sci Eng A 459:375
33. Tanaka Y, Kajihara M (2007) Mater Sci Eng A 459:101
34. Griger A, Stefániay V, Turmezey T (1986) Z Metallkde 77:30